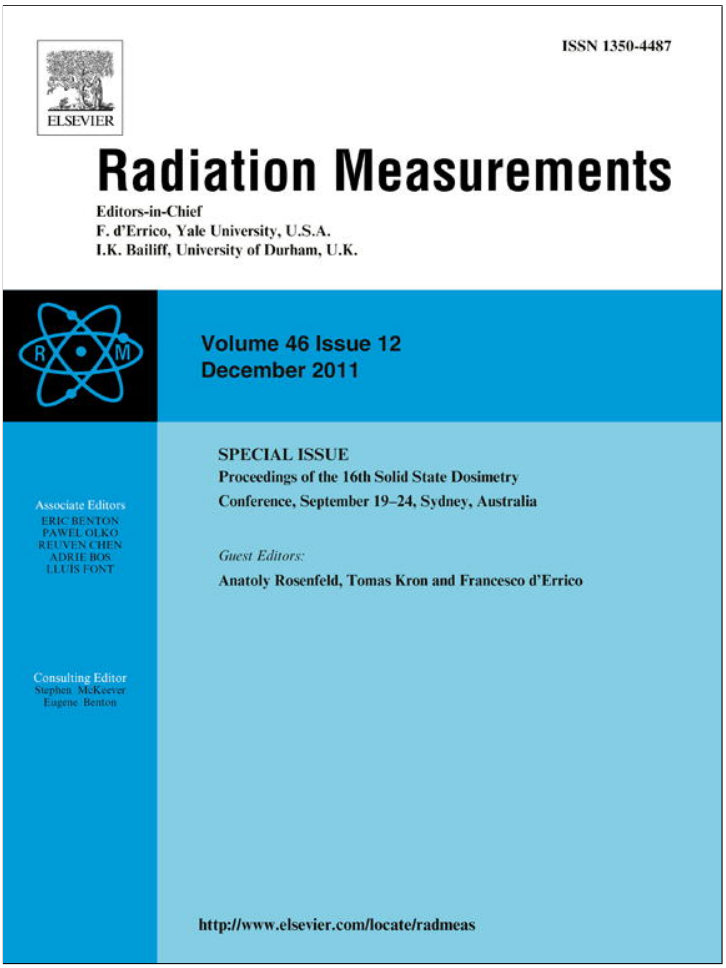

Radiation Measurements 46 (2011) 1765–1769

Contents lists available at ScienceDirect

Radiation Measurements

journal homepage: www.elsevier.com/locate/radmeas

Studies of the neutron field of the Energy plus Transmutation set-up under 4 GeV deuteron irradiation

J.J. Borger [a], S.R. Hashemi-Nezhad [a,*], D. Alexiev [b], R. Brandt [c], W. Westmeier [c], B. Thomauske [d], S. Tiutiunikov [e], M. Kadykov [e], V.S. Pronskikh [e], J. Adam [e]

[a] Institute of Nuclear Science, School of Physics, A28, University of Sydney, NSW 2006, Australia
[b] The Australian Nuclear Science and Technology Organisation, Locked Bag 2001, Kirrawee NSW 2232, Australia
[c] Kernchemie Institute, Philipps-Universität, 35032 Marburg, Germany
[d] Forschungszentrum Jülich, ISR-6, 52425 Jülich, Germany
[e] Joint Institute for Nuclear Research, 141980 Dubna, Russian Federation

ARTICLE INFO

Article history:
Received 10 November 2010
Received in revised form
21 April 2011
Accepted 30 April 2011

Keywords:
Accelerator Driven Systems, ADS
Deuteron beam
MCNPX
Bismuth activation

ABSTRACT

The Energy plus Transmutation (EPT) set-up of the Joint Institute of Nuclear Research (JINR), Dubna, Russia is composed of a lead spallation target surrounded by a blanket of natural uranium. The target was irradiated with 4 GeV deuterons. Rates of reactions leading to the production of ^{206}Bi from ^{209}Bi were determined through gamma spectrometry. These were compared with calculated reaction rates determined using the MCNPX code, including the INCL4 intranuclear cascade and ABLA fission/evaporation models along with available cross section data. Close agreement was found for the production of ^{206}Bi. The high threshold energy of neutron induced production indicates that neutrons causing these reactions are most likely to originate in the intranuclear cascade phase of the interaction. This is therefore an important reaction for validation of the computational models used.

1. Introduction

Future Accelerator Driven Systems (ADS) (Carminati et al., 1993) will rely upon spallation neutrons (produced in a heavy metal target under the bombardment of high energy light ions) to sustain fission within a sub-critical core. The maximum energy of neutrons seen in ADS stretches to the energy of the incident ions (GeV energy range). Understanding this high energy neutron region has implications for all reaction rates within reactor materials, and requires Monte Carlo models which can accurately simulate such spectra. It is the aim of this paper to provide a check of this accuracy through the use of ^{206}Bi activation in bismuth samples placed in the Energy plus Transmutation (EPT) experimental set-up.

The EPT set-up (Fig. 1a and b) consists of a central cylindrical natural lead target surrounded by a blanket of natural uranium rods and a reflecting volume of granulated polyethylene. A full description of the set-up is available elsewhere (Hashemi-Nezhad et al., 2008 and refs therein). A beam of incident light ions (in the present case 4 GeV deuterons) is normally incident on the front face of the central target. The beam interactions in the target induce spallation reactions, emitting neutrons which are multiplied by fission in the surrounding blanket.

The set-up is constructed in four sections with gaps in between them (see Fig. 1b), allowing samples to be placed around and within the structure of the set-up. These samples provide information on the spectral and spatial distribution of neutrons produced by spallation in the target and fission in the blanket.

2. Experimental method

2.1. Activation samples

Six 0.25 mm thick samples of Bismuth foil (Goodfellow 99.999% purity) were sandwiched between ~50 μm layers of mica, used to record fission tracks (not discussed in the present paper). These samples were placed in a gap between the first two sections of the target/blanket assembly. The samples were positioned along a radius rotated to the right 30° from the vertical (as seen by the incident beam) and spaced at radial distances of $\rho = 0$, 3, 6, 8.5, 11 and 13.5 cm from the target axis (see Fig. 1c). As well as fission events, these samples were also subject to other interactions which

* Corresponding author. Tel.: +61 2 9351 5964; fax: +61 2 9351 7726.
E-mail address: reza@physics.usyd.edu.au (S.R. Hashemi-Nezhad).

1350-4487/$ – see front matter © 2011 Elsevier Ltd. All rights reserved.
doi:10.1016/j.radmeas.2011.04.037

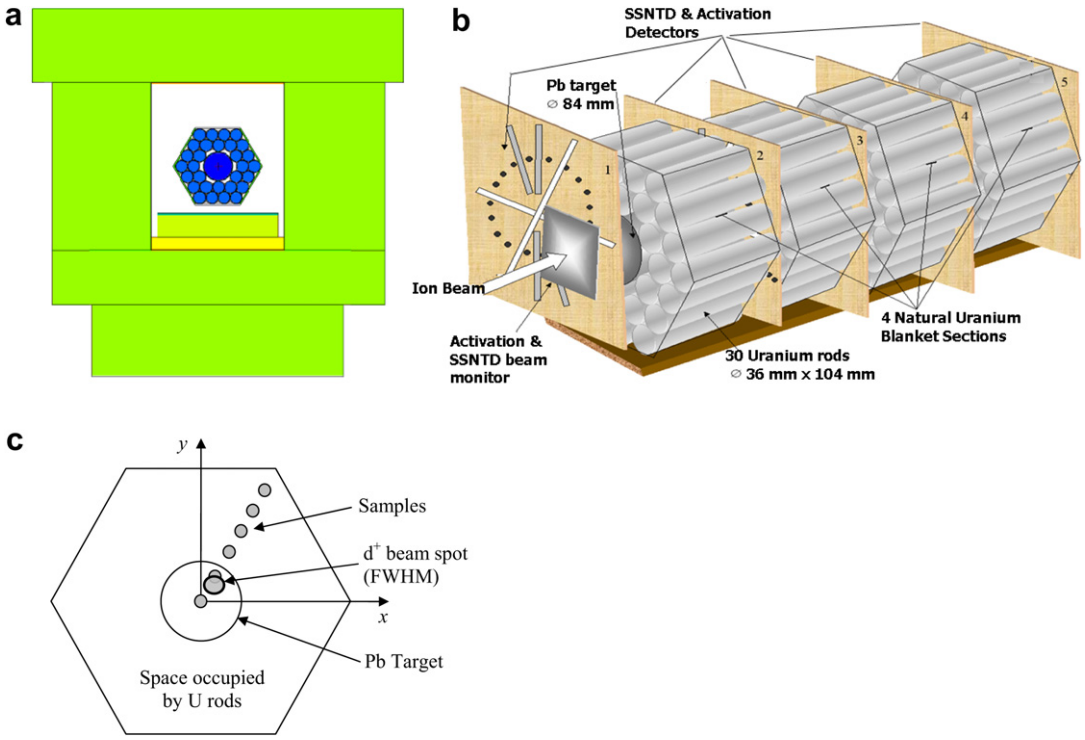

Fig. 1. Views of the EPT set-up: a) Cross section of the EPT set-up modelled in MCNPX. The target is surrounded on four sides by a 1 mm layer of cadmium and a thick shield of polyethylene. b) the arrangement of blanket sections and samples in the set-up, c) The arrangement of bismuth activation samples in plate 2, between the first and second blanket sections and the position and shape of the beam spot.

can be useful in understanding the neutron field via gamma spectrometry. In order for a reaction to be useful, it must:

1) probe the high energy region of the neutron spectrum;
2) have a significant known cross section in this energy range;
3) have a radioactive product;
4) have a product half life *short enough* to allow fast product build up in low intensity irradiation, and
5) have a product half life *long enough* to allow convenient measurement of samples in the time available after irradiation.

In the case of bismuth samples, only the ^{209}Bi(n,4n)^{206}Bi reaction satisfies all these criteria.

2.2. Irradiation procedure

The EPT set-up was irradiated with pulsed 4 GeV deuterons from the NUCLOTRON accelerator of the Joint Institute of Nuclear Research (JINR) over a period of some 18 h. As seen in Fig. 2, the magnitude of each pulse varies significantly over the duration of the irradiation period and there were significant periods during which no beam was available.

In light of this, it is necessary to develop a correction factor relating the activity induced by the variable and intermittent irradiation to an equivalent constant irradiation.

The activity of a sample at the end of a constant irradiation A, over irradiation time t_{irr} is given by

$$A = R_C[1 - \exp(-\lambda t_{irr})],$$

where R_c is the equivalent constant reaction rate, and λ is the decay constant for the induced activity.

In a pulsed irradiation, activity A_i is produced in each pulse i (with rate R_i and length t_{pi}), and then decays over the remaining irradiation time t_{di}

$$A_i = R_i[1 - \exp(-\lambda t_{pi})]\exp(-\lambda t_{di}).$$

The total induced activity is then the sum over the activities from all pulses. The correction for an intermittent or pulsed irradiation is then

$$P = \frac{R_C[1 - \exp(-\lambda t_{irr})]}{\sum_{i=1}^{n} R_i[1 - \exp(-\lambda t_{pi})]\exp(-\lambda t_{di})}$$

The reaction rate during one pulse R_i, relative to the mean reaction rate for the whole irradiation R_C is given by

$$\frac{R_i}{R_C} = \frac{t_{irr}\Phi_i}{t_{pi}\sum_{i=1}^{n}\Phi_i} = \frac{t_{irr}}{t_{pi}}W_i,$$

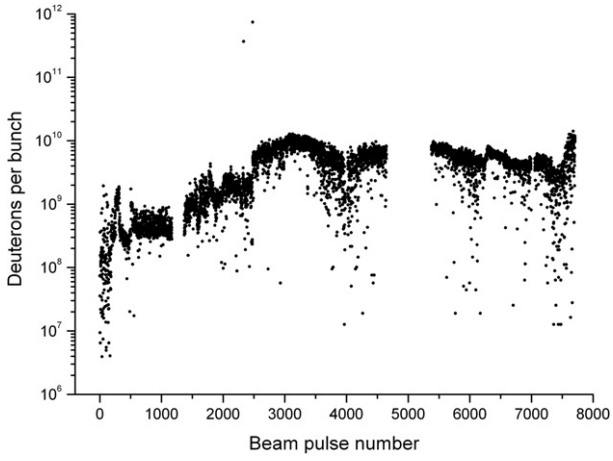

Fig. 2. Variation of deuteron beam intensity during the irradiation as provided by the NUCLOTRON operators.

where Φ_i is the time integrated fluence of pulse i and t_{irr} is the total irradiation time, whilst W_i is the relative strength of each pulse to the total fluence. Then the pulsed irradiation correction is

$$P = \frac{1-\exp(-\lambda t_{irr})}{t_{irr}\sum_{i=1}^{n}\frac{1}{t_{pi}}W_i[1-\exp(-\lambda t_{pi})]\exp(-\lambda t_{di})}.$$

If each pulse is short compared to the half life of the induced activity, then the following approximation can be made:

$$[1-\exp(-\lambda t_{irr})] \cong \lambda t_{pi} \text{ for } t_{pi} << t_{1/2}.$$

Then the correction for isotopes with half lives long compared to the length of the individual pulses can be reduced to

$$P \cong \frac{1-\exp(-\lambda t_{irr})}{t_{irr}\sum_{i=1}^{n} W_i \lambda \exp(-\lambda t_{di})}.$$

Since the half life of the induced activity (^{206}Bi) is 6.24 days and pulses much shorter than 1s are expected, this simplification is expected to hold in the present case.

2.3. Beam position on the target

In the initial set-up prior to irradiation, the target axis was carefully aligned with the beam axis. However, the beam position, determined after the irradiation by activation and track detector techniques, was found to lie some distance away from the axis of the lead target. A significant shift in beam position had taken place at some time during the irradiation. This probably occurred during one of the interruptions of the beam, shown in Fig. 2. The mean position and FWHM of the beam are presented in Table 1 and visible in Fig. 1c.

2.4. Detector characterisation and activity measurement

The activities of ^{206}Bi induced in each of the six samples were measured by gamma spectrometry using an ORTEC GLP-36360/13 planar HPGe detector. Samples were counted for up to 13 h each within the first week following the end of the irradiation. Sample activity was determined from the full energy peak (FEP) counts corresponding to the 183.977 keV gamma line.

Since the sample activities were weak, close source-detector geometry was required for adequate statistics. However, at close geometries, coincidence summing can have a significant effect on the number of counts in the FEP (Debertin and Helmer, 1988). This effect requires correction in determining the sample activity and detector FEP efficiency.

Summing-out of the FEP is due to the gamma of interest being detected in coincidence with another gamma from the same cascade. This results in the loss of a count from the FEP. Correction for this effect only requires the knowledge of the detector total efficiency since the second coincident gamma does not have to be detected at full energy for this to occur.

Table 1
Irradiation details.

Location	NUCLOTRON acceleration, Joint Institute of Nuclear Research (JINR), Dubna, Russian Federation.
Incident particle	Deuteron
Incident energy	4 Ge V
X co-ordinate of beam[a]	2.4 cm right from centre (FWHM 2.1 cm)
Y co-ordinate of beam[a]	1.7 cm up from centre (FWHM 1.8 cm)

[a] Refer to Fig. 1c.

On the other hand *summing-in* to the FEP is caused by two gammas, whose energy sum is equal to the energy of the peak of interest (such as in the case of cross-over transitions), being detected in coincidence and at full energy. This leads to a gain of a count to the FEP. Correcting for summing-in effects requires prior knowledge of the detector FEP efficiency. Therefore gamma lines, for which significant summing-in is possible, were not included in the FEP efficiency determination.

Spectra were taken with the available standard point sources ^{152}Eu, ^{54}Mn, ^{113}Sn, ^{139}Ce, ^{137}Cs, ^{241}Am, ^{57}Co and ^{133}Ba. Of these sources, ^{241}Am, ^{57}Co, ^{139}Ce, and ^{137}Cs can be considered as approximately mono-energetic and it is therefore possible to characterise the detector's total efficiency at the energies 59.54, 123.66, 165.86 and 661.66 keV. However, in order to obtain an accurate total efficiency curve to suit the energy range of interest, more information is required.

Monte Carlo simulations of the source-detector geometry (Edwards, 2010) were carried out using the MCNPX 2.5.0 (Pelowitz, 2005) code for photon energies at and between those mentioned above, to generate a detector total efficiency curve. Good agreement was found between the total efficiency points determined experimentally with that determined via simulation (see Fig. 3).

Coincidence corrections were calculated for selected peaks of the ^{152}Eu, ^{54}Mn, ^{113}Sn, and ^{133}Ba sources using a matrix method (Bikit et al., 2009; Novkovic et al., 2007; Semkow et al., 1990). By this method all transition paths from parent ground state to daughter ground state are considered including coincidences of the type $\gamma+\gamma$ and $\gamma+X$. The largest correction required was about 14%. The uncertainties of these factors are due mainly to the uncertainty in the detector total efficiency, and the daughter fluorescence yields. These equate to less than a few percent.

With the use of these corrections and the FEP counts of the selected energies, the corrected full peak efficiency was determined, and a fitted curve was obtained (Fig. 3). In the energy region of interest ($E_\gamma \geq 150$ keV) the uncertainty in the full energy peak efficiency is found to be not more than 3%.

A further correction factor was also required to take into account the difference in sample geometry between the standard point sources and the bismuth samples, which were thick square foils. Again, MC simulations were used to correct for the different sample geometry and to account for the material self-shielding characteristics. Each correction fell in the range (0.962–0.964) ± 0.16% depending on the dimensions of each foil. The uncertainty obtained is a result of MC statistics.

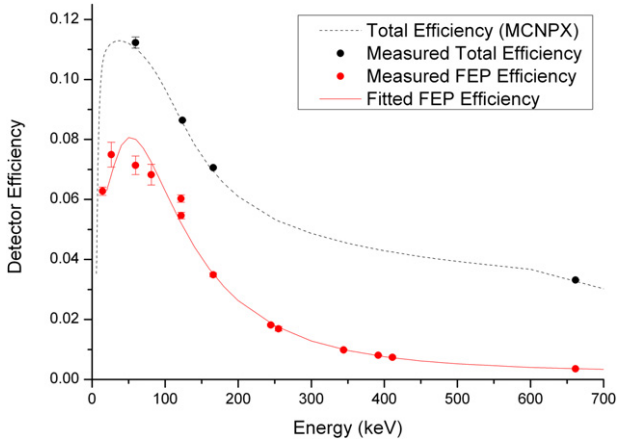

Fig. 3. ORTEC GLP-36360/13 HPGe detector total efficiency and full energy peak (FEP) efficiency curves.

3. Monte Carlo simulations of ^{206}Bi production

The EPT set-up and relevant samples were modelled using the MCNPX 2.5.0 code (Pelowitz, 2005), including the INCL4 intranuclear cascade (Boudard et al., 2002) and ABLA fission-evaporation models (Gaimard and Schmidt, 1991) for high energy interactions. The la150n (neutron) and la150h (proton) libraries (Chadwick et al., 1999) were also used where available. The measured mean beam position and shape was taken into account and all samples (including those not discussed here) were placed within the simulated set-up.

To calculate the production of ^{206}Bi in the set-up, experimentally determined data for the ^{209}Bi(n,4n) ^{206}Bi (Kim et al., 1998), ^{209}Bi(p,x) ^{206}Bi (Kuhnhenn, 2001; Michel et al., 2002), and ^{209}Bi(d,x) ^{206}Bi (Gonchar et al., 1994) reactions were used. Such cross sections are only known at discrete energies, so neutron, proton and deuteron fluence in the energy ranges of interest were binned such that the discrete cross section values lay at the midpoints of the energy bins. The fluence in each bin was then directly multiplied with its corresponding cross section value. For neutron induced reactions, the cross section is known only for energies $E_n \leq 150$ MeV. The cross section was assumed to be constant above 150 MeV.

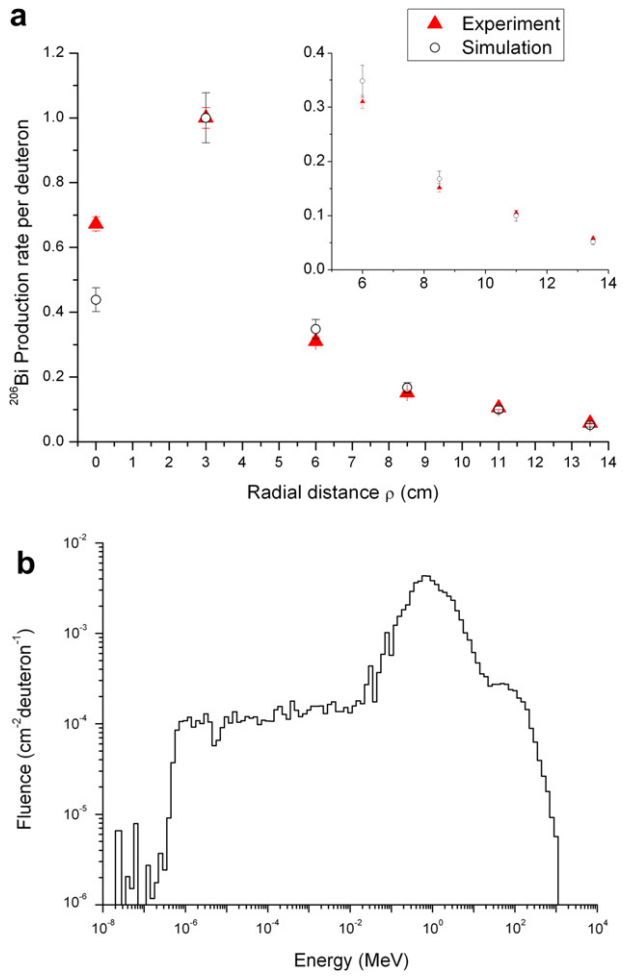

Fig. 4. (a) Radial distribution of ^{206}Bi production in plate 2 of the EPT set-up. Experimental and simulated results are normalised to the data point at $\rho = 3$ cm. The radial distance ρ was measured from the target axis. The inset highlights samples with $\rho \geq 6$ cm. There is excellent agreement between the experiment and simulation for samples with $\rho \geq 3$ cm. (b) Typical neutron spectrum in a sample at $\rho = 13.5$ cm.

Table 2
Proportions of ^{206}Bi production attributable to different incident particles.

Radial distance ρ (cm)	^{206}Bi production induced by:		
	Neutron (%)	Proton (%)	Deuteron (%)
0	95.2	4.5	0.3
3	84.1	8.1	7.8
6	95.5	4.5	0.0
8.5	97.3	2.7	0.0
11	98.1	1.9	0.0
13.5	99.0	1.0	0.0

4. Results and discussion

The normalised radial distribution of the ^{206}Bi production rate is shown in Fig. 4. Close agreement is found between the measured and simulated reaction rates for all samples with $\rho \geq 3$ cm. For the sample at $\rho = 0$ cm the measured reaction rate is found to be 56% higher than the rate determined via simulation. It is possible that the beam may have been in the central position for a significant (early) proportion of the beam time before the beam shift occurred, leaving an elevated activity in the sample at $\rho = 0$ cm. The simulation could only use the known mean beam position in determining the activity.

In the Monte Carlo calculation of the production rate of ^{206}Bi it is possible to separate the rate into neutron, proton and deuteron induced components. Table 2 shows the proportion of ^{206}Bi production attributed to incident neutrons, protons and deuterons. It is clear that only samples which overlap with the direct beam (such as at $\rho = 3$ cm) are subject to significant deuteron induced reactions whilst only those on or near the beam ($\rho = 0$, 3 and 6 cm) are subject to significant proton induced contributions. The samples placed at $\rho = 8.5$ cm 11 cm and 13.5 cm away from the target axis are subject almost entirely to neutron induced reactions. The threshold energy for the ^{209}Bi(n,4n) ^{206}Bi reaction is 22.5 MeV, which is far above the energy of neutrons generated by fission or evaporation processes and therefore accessible only by neutrons emitted in the intranuclear cascade. The observed apparent agreement between the experimental and calculated results forms a validation of the INCL4/ABLA models used in the simulations.

5. Conclusions

The Energy plus Transmutation set-up was irradiated with 4 GeV deuterons and the radial variation of the fast neutron density ($E_n > 22.5$ MeV) was elucidated using bismuth foils and an activation technique. Taking into account the neutron, proton and deuteron induced reactions, good agreement is found between the measured and simulated rates of ^{206}Bi production in the set-up using MCNPX with the INCL4/ABLA cascade and available cross sections. It is expected that full agreement could be obtained if it were possible to take time variation of the beam position into account.

The ^{209}Bi(n,4n)^{206}Bi reaction has a threshold of 22.5 MeV, above the neutron emission energies possible in either evaporation or fission processes. This reaction, therefore, provides a check of the cascade model (INCL4) used in the simulation. The good agreement found here is evidence of the ability of such codes to successfully model Accelerator Driven Systems.

References

Bikit, I., Nemes, T., Mrda, D., Jovancevic, N., 2009. On the absolute source activity measurement with a single detector: the Ba-133 case. Nucl. Instrum. Meth. Phys. Res. A 612, 103–111.

Boudard, A., Cugnon, J., Leray, S., Volant, C., 2002. Intranuclear cascade model for a comprehensive description of spallation reaction data. Phys. Rev. C 66, 044615.
Carminati, F., Klapisch, R., Revol, J.P., Roche, C., Rubio, A., Rubbia, C., 1993. An Energy Amplifier for Cleaner and Inexhaustible Nuclear Energy Production Driven by a Particle Beam Accelerator. CERN.
Chadwick, M.B., Young, P.G., Chiba, S., Frankle, S.C., Hale, G.M., Hugher, H.G., Koning, A.J., Little, R.C., MacFarlane, R.E., Prael, R.E., Waters, L.S., 1999. Cross section evaluations to 150 MeV for accelerator-driven systems and implementation in MCNPX. Nucl. Sci. Eng. 131, 293–328.
Debertin, K., Helmer, R.G., 1988. Gamma- and X-Ray Spectrometry with Semiconductor Detectors. Elsevier Science, Amsterdam.
Edwards, V., 2010. Private Communication. Nucletron Pty. Ltd., Sydney.
Gaimard, J.-J., Schmidt, K.-H., 1991. A Re-examination of the abrasion-ablation model for the description of the nuclear fragmentation reaction. Nucl. Phys. A 531, 709–745.
Gonchar, A.V., Kondratev, S.N., Lobach, Y.N., Nevskiy, S.V., Sklyarenko, V.D., Tokarevskiy, V.V., 1994. Integral cross sections for (d, xn) and (d, pxn) reactions on Bi-209 nuclei at deuteron energy range to 47MeV. Ross. Akad. Nauk Izv. Energ 58, 81.
Hashemi-Nezhad, S.R., Zhuk, I., Kievets, M., Krivopustov, M.I., Sosnin, A.N., Westmeier, W., Brandt, R., 2008. Determination of natural uranium fission rate in fast spallation and fission neutron field: an experimental and Monte Carlo study. Nucl. Instrum. Meth. Phys. Res. A 591, 517–529.
Kim, E., Nakamura, T., Konno, A., Uwamino, Y., Nakanishi, N., Imamura, M., Nakao, N., Shibata, S., Tanaka, S., 1998. Measurements of neutron spallation cross sections of C-12 and Bi-209 in the 20–150 MeV energy range. Nucl. Sci. Eng. 129, 224–245.
Kuhnhenn, J., 2001. Thin Target Cross Sections for Proton-Induced Production of Radionuclides from Lead and Bismuth Over the Proton Energy Range from 9 to 71 MeV. Universität Köln, Köln.
Michel, R., Gloris, M., Protoschill, J., Herpers, U., Kuhnhenn, J., Sudbrock, F., Malmborg, P., Kubik, P., 2002. Cross sections for the production of radionuclides by proton-induced reactions on W, Ta, Pb and Bi from thresholds up to 2.6 GeV. J. Nucl. Sci. Tech. Suppl. 2, 242.
Novkovic, D., Kandic, A., Durasevic, M., Vukanac, I., Milosevic, Z., Nadderd, L., 2007. Coincidence summing of X- and gamma rays in gamma ray spectrometry. Nucl. Instrum. Meth. Phys. Res. A 578, 207–217.
Pelowitz, D.P., 2005. MCNPX User's Manual: Version 2.5.0. Los Alamos National Laboratory and University of California.
Semkow, T.M., Mehmood, G., Parekh, P.P., Virgil, M., 1990. Coincidence summing in gamma-ray Spectroscopy. Nucl. Instrum. Meth. Phys. Res. A 290, 437–444.